Red-shift Due to Pump Intensity in Er:ZBLALiP Whispering Gallery Mode Lasers

Patrice Feron, Zhiping P. Caï, Huiying Y. Xu, Guy Stephan, P. Goldner, Michel Mortier

Red-shift due to pump intensity in Er:ZBLALiP Whispering-gallery mode lasers

Patrice Féron[a], Zhiping Cai[b], Huiying Xu[c], Guy M. Stéphan[a]
Philippe Goldner[d], Michel Mortier[d]

[a]GIS "FOTON" Laboratoire d'Optronique (CNRS-UMR 6082)
6 rue de Kerampont, 22300 Lannion, France
[b]Department of Physics, University of Xiamen, Xiamen 361005, China
[c]Department of Electric Engineering, University of Xiamen, Xiamen 361005, China
[d]Groupe d'Optique des Terres Rares, (CNRS-UMR 7574)
1 place Aristide Briand, 92190 Meudon, France

ABSTRACT

A new kind of Erbium doped heavy fluoride glass Er:ZBLALiP has been studied. Microspheres were fabricated with this fluoride glass. Whispering Gallery Mode laser spectra around 1550 nm were analyzed for different sphere diameters and Erbium concentrations (from 0.01 % to 0.2 % by mole) under pumping by a fiber taper at 1480 nm. Red-shift effect on the frequencies of both fluorescence and laser spectra is experimentally observed when the pump power is increased, originating from thermal effects. A spectroscopic technique based on the green upconversion fluorescence is used to compute a loading effective temperature for the Er:ZBLALiP microsphere and this further allows us to calibrate the properties of the microsphere laser in terms of the thermal expansion as well as the variation of the refractive index.

Keywords: Whispering Gallery Mode lasers, Erbium doped fluoride glass, Erbium concentration , Temperature effect, Line shift

1. INTRODUCTION

With recent breakthrough in terms of output power, the Erbium 3 μm fiber laser has become an object of intense scientific research and an increasingly attractive tool for applications.[1] In other respects, since a few years optical microspherical cavities are subject to numerous studies.[2] In dielectric spheres light can be guided through high-Q whispering-gallery-modes (WGMs). The unique combination of strong temporal and spatial confinement of light makes these systems of interest for a number of applications as diverse as quantum optics[3] and optical communications.[4] Among these, rare earth doped glass have been demonstrated as potentially compact laser source.[5–7]

In this frame, a new fluoride glass composition allowing easy incorporation of rare earth ions and revealing an improved stability with regard to classical fluorozirconate glasses enabling easier shaping as fiber making or microsphere fabrication with a weaker nucleation risk has been studied.

We present experimental results on microspherical laser at 1550 nm pumped at 1480 nm using half-taper for direct fiber coupling. Our experiments are focused on the transition ${}^4I_{13/2} \longrightarrow {}^4I_{15/2}$ at 1550 nm of Er:ZBLALiP spheres, which offers potential applications in telecommunications. We have made experiments on different glass samples with doping rate in Erbium varying from 0.01 $mol.\%$ to 6 $mol.\%$. Laser oscillations were obtained for different Erbium concentrations (from 0.03 $mol.\%$ to 0.2 $mol.\%$). Red-shift effect on the wavelengths of both fluorescence and laser spectra was experimentally observed when the pump power was increased, originating from thermal effects. A spectroscopic technique based on the green upconversion fluorescence is used to precisely compute a loading effective temperature for the Er:ZBLALiP microsphere, and this further allows us to calibrate

Further author information: (Send correspondence to Patrice Féron or Michel Mortier)
Patrice Féron: E-mail: patrice.feron@enssat.fr, Telephone: +33 (0)2 96 46 66 42, Fax : +33 (0)2 96 46 66 75
Michel Mortier: E-mail: michel.mortier@cnrs-bellevue.fr, Telephone +33 (0)1 45 07 53 00, Fax : +33 (0)1 45 07 51 07

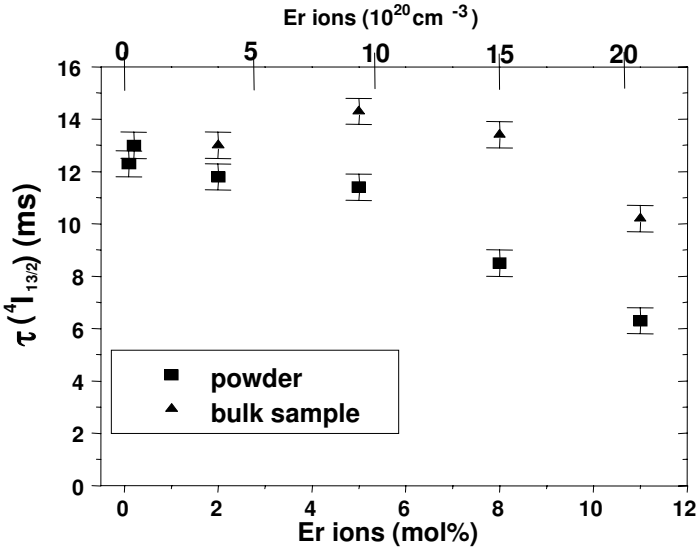

Figure 1: Lifetime of the $^4I_{13/2}$ level *vs* Erbium concentration for bulk and powder

the properties of the microsphere laser in terms of the thermal expansion as well as the variation of the refractive index.

2. EXPERIMENT

2.1. Er:ZBLALiP glass

Glasses with composition in $mol.\%$ $62.2ZrF_4, 19.5BaF_2, 6.1LaF_3, 2.4LiF, 6.1PbF_2$ have been prepared by melting of the powders (commercial raw materials of purity higher than 99.99%) in a covered platinium crucible at about $800°C$ for 45 min in a dry argon glove box with a water content lower than $5ppm$. The melt was poured in a preheated copper mould at $250°C$ and slowly cooled down to room temperature. The doping ion is added in excess to the formula $+xErF_3$ where x is the Erbium doped concentration in $mol.\%$. Several concentration ranging from $x = 0.01$ $mol.\%$ to 11 $mol.\%$ were prepared, corresponding to 0.02 to $22 \times 10^{20} Er\ ions/cm^3$. The samples obtained are of good optical quality.
Differential Thermal Analysis (DTA) was done[8] for 0.01, 2 and 11 $mol.\%$ of Erbium ions. The melting peak is centered around $530°C$ independently of the Erbium content. The glass transition temperature lies respectively at $247°C$, $251°C$ and $268°C$. The interval between T_g and T_x is equal to respectively 76, 88 and $86°C$.
The fluorescence decay of Er^{3+} ions were recorded after excitation by a pulsed frequency doubled Nd:Yag laser at 532 nm. The lifetime of the $^4I_{13/2}$ level corresponding to the 1550 nm transition has been measured on bulky and powdered samples (Fig.1). For the low doping rate, *i.e* less or equal to 0.2% no significant difference is detected between the two measurements of a same composition. However, when the doping rate reaches or exceeds 2% an increasing lengthening of the lifetime measured on bulky samples is observed with respect to the powdered samples when the concentration is increased.
Absorption cross section were recorded on a double-beam Cary 17 spectrometer with a resolution better than 0.1 nm. Figure 2.a presents the absorption cross section for the $^4I_{15/2} \longrightarrow^4 I_{13/2}$ transition. This was experimentally measured in an Er:ZBLALiP bulk chip 0.05 $mol.\%$ Erbium doped and the emission cross section spectrum was derived using the McCumber's theory.[9] The absorption and emission cross sections are related by

$$\sigma_a(\lambda) = \sigma_e(\lambda) \cdot \frac{Z_L}{Z_U} \exp[\frac{hc}{k_B T}(\frac{1}{\lambda} - \frac{1}{\lambda_0})] \quad (1)$$

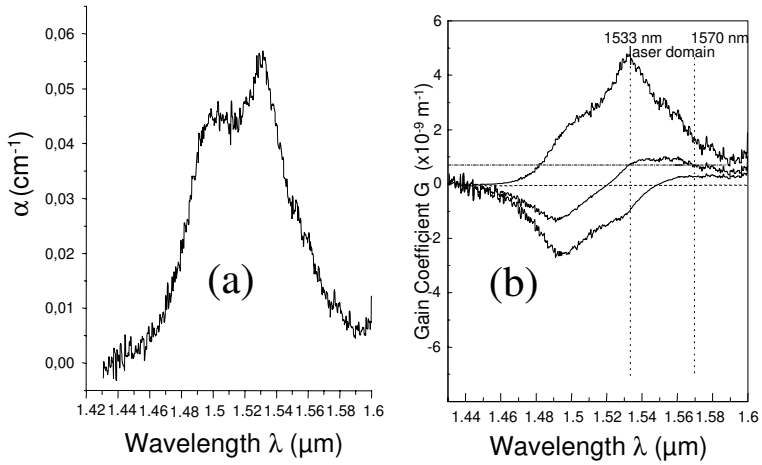

Figure 2: (a) Absorption Spectrum (b) Gain Spectra for ZBLALiP glass Erbium doped 0.05 $mol\%$

where Z_L, Z_U are the partition functions of the upper and lower levels, λ_0 the wavelength corresponding to the two lowest Stark levels of the ${}^4I_{13/2}$ and ${}^4I_{15/2}$ levels. h is the Planck's constant, c the light velocity, k_B the Boltzmann's constant and T the temperature in degrees Kelvin. Computation of Z_L, Z_U needs the spectroscopic values of both levels of Erbium ion, *i.e.* their degenerencies and Stark-level energies (see Eq.2 in Ref. 9). In general, such Stark components of Er^{3+} doped glasses can be deduced from the low temperature absorption-emission spectra.[10] Based on these absolute cross section spectra, the net gain spectra $G(\lambda, p)$ can be computed in terms of the pumping level[11] as the following:

$$G(\lambda, p) = n_{Er} \cdot [p\sigma_e(\lambda) - (1-p)\sigma_a(\lambda)] \tag{2}$$

where p is the fractional factor of the excited Erbium ions in the metastable level ${}^4I_{13/2}$. It is important to note that p is an excitation parameter averaged over temperature due to Stark effects of both the upper and lower levels. $G(\lambda, p)$ represents the gain spectra at room temperature which is applicable to the lasing threshold condition where there is no significantly increase of temperature. Figure 2.b represents the gain spectra calculated for several values of p. We note a laser domain extending from 1533 to 1570 nm.
Spheres were produced by fusion of fluoride glass powders with a microwave plasma torch. Powders are injected axially and melt when passing through the flame. Superficial tensions giving them their spherical form. Free microspheres with a diameter which varies from 10 to 200μm are collected a few centimeters below. Then, they are glued at a stretched tip of optical fibers (20μm in diameter) which allows to manipulate them easily and to insert them in the optical setup.

2.2. Experimental Setup

A WGM is described by a polarization (TE or TM) and three quantum numbers (n, l, m) which represent the radial, angular and azimuthal mode numbers, respectively. To excite High-Q WGMs (lowest n), light has to be launched from a phase-matched evanescent wave in an adjacent waveguide or a prism under total internal reflection. For microspherical lasers, most of couplings have been realized by free beams,[5] prisms,[6,7] tapers[12,13] and half tapers.[14,15] Among the different pumping wavelengths which can be used with Erbium doped glasses[16] (810 nm, 975 nm and 1480 nm) we chose 1480 nm to obtain a good overlap between the pump and laser mode volumes in the microsphere and to optimize the lasing process in our system. It presents also

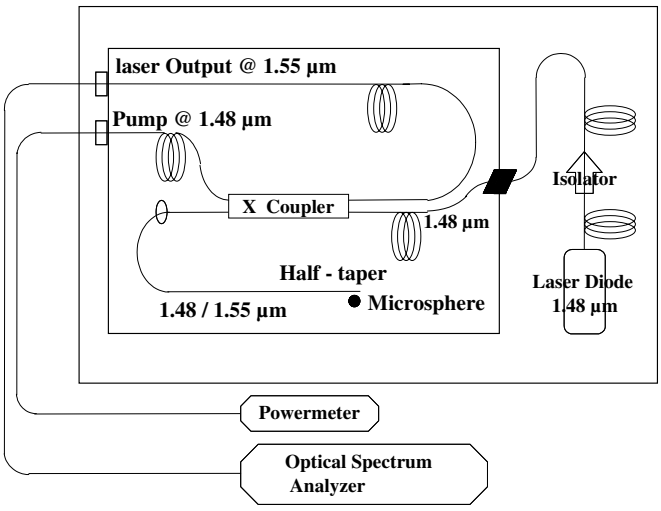

Figure 3: Experimental setup

advantages when coupling is obtained using one single half-taper as the pump wavelength is close enough to that of the laser field, such coupling device allows to couple both fields in and out the microspherical laser. The fiber coupling experiments were performed with half-tapered fiber, that we obtained by heating and stretching standard telecommunication fiber (single mode at 1.55 μm) until breaking, using a fusion optical splicing system. The drawn length was typically 850 μm, and the taper end reduced to 1.5 μm in diameter. The experimental Setup (see Fig.3) was realized with standard fiber-optic components spliced or connected with APC connectors. Mounting Er:ZBLALiP spheres on microtranslations brought the equator region in contact with the evanescent field surrounding the taper. The pump device was based on a multimode-fiber laser diode (maximum outpout power, 100 mW) operating at 1.48 μm, an isolator that prevent feedback into the laser diode, and an X-coupler at 1.48-1.55 μm. The X-coupler allowed us to use the same fiber to pump and to collect the fluorescence or the laser signal. The X-coupler enabled us to have a pump reference that was separated from the laser signal, which was analyzed with a 0.1 nm resolution optical spectrum analyzer (OSA).

2.3. Results

For any sphere diameter and doping concentration, the optical spectrum of the laser below the threshold show an enhancement of the fluorescence intensity and a higher peak density than those obtained with a prism as demonstrated in a previous paper.[14] More modes can thus be excited in the sphere, which qualitatively justifies the large number of lines (Fig.4). Nevertheless, for sufficiently large sphere diameter in respect to the wavelength we can use an analysis similar to that used for excitation by a prism for the fluorescence spectra[7] on the basis of asymptotic expressions[17] for WGM size parameters. This standard analysis shows that these series of peaks can be assigned to several families of modes instead of one predominant family when a prism is used, each of them having the same radial order n but different polarizations and angular momenta l. When increasing the pump intensity we obtained laser oscillation.
Figure 4 shows the evolution of WGMs spectra for a 0.05 $mol.\%$ Erbium doped microsphere with a diameter of 60 μm as the pump intensity increased (denoted by LD driven current). At 100 mA excitation, the emission spectrum exhibits a typical discrete WGMs feature (fig.4a), at threshold (110 mA (fig.4b) we observed laser oscillation at 1550.2 nm (corresponding to a maximum of the gain spectrum) and for an high pumping rate (fig.4c) we obtained multimode laser emission lines. For other doping rate, we obtained similar behaviour differing by the threshold and the laser domain. We studied several samples with different concentration in

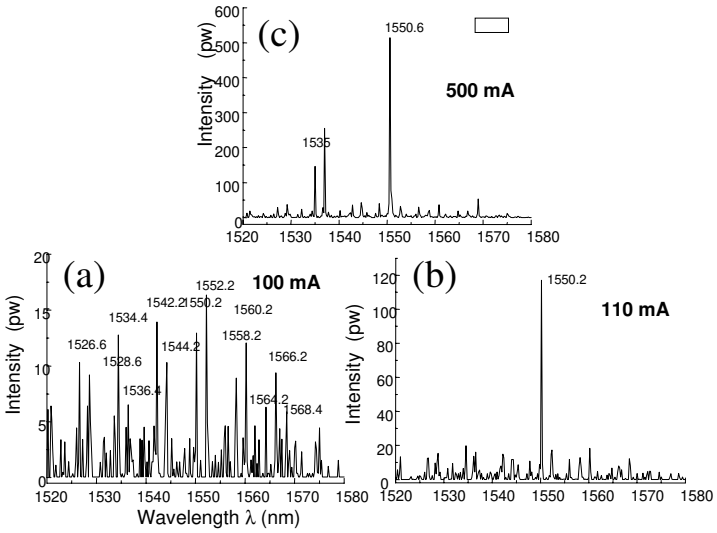

Figure 4: (a)Fluorescence spectrum - laser spectrum (b) at threshold (c) at $\sim 5\times$ threshold

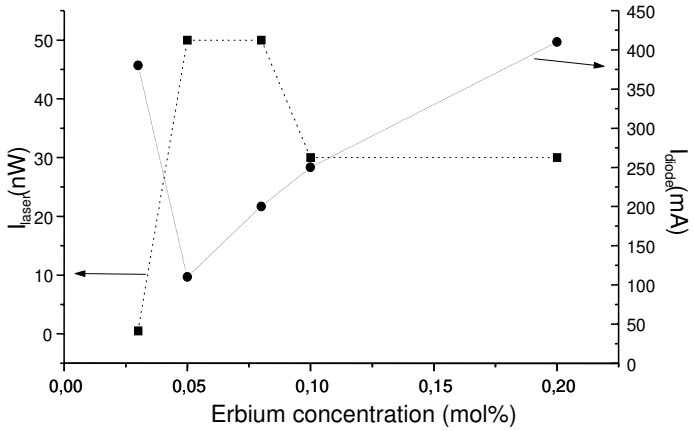

Figure 5. squares- Main WGM laser line intensity. Dots- driven current of the diode pump at threshold *vs* Erbium concentration

Erbium. For every doping rate we tested about ten spheres. Laser oscillation was obtained for concentrations equal to 0.03 $Mol.\%$, 0.05 $Mol.\%$, 0.08 $Mol.\%$, 0.1 $Mol.\%$, 0.2 $Mol.\%$ with an optimal concentration between 0.05 $Mol.\%$ and 0.08 $Mol.\%$. The evolution of the threshold and of the laser intensity are plotted versus the doping rate on figure 5 (dotted lines are just guides for the eyes). Such concentrations lead to : an extended laser domain, a lower threshold and a better efficiency than other concentrations. Doping rate too low (0.01 $Mol.\%$) or too high (2 $Mol.\%$ and 6 $Mol.\%$) does not allow laser oscillation.

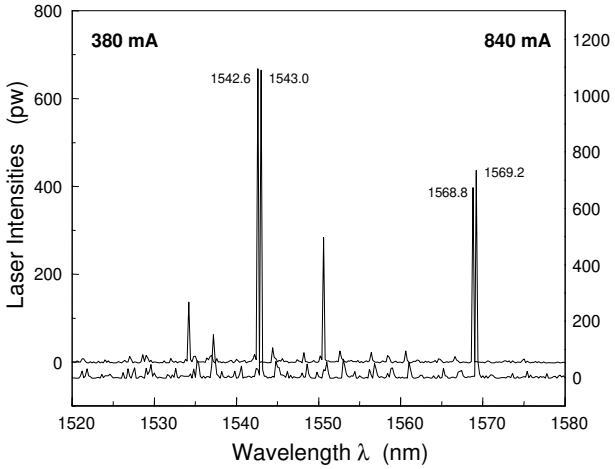

Figure 6: Red-Shift of WGM laser spectra of Er:ZBLALiP (0.05 mol.%) 2a = 60 μm.

2.4. Red shift effect on laser lines

The laser spectra were analyzed by an Optical Spectrum Analyzer with a resolution of 0.1 nm as the pump power was increased under 1480 nm pumping, and typical results are illustrated in Fig.6. The two wavelengths at 1542.6 nm and 1568.8 nm, when the pump intensity is under 380 mA shift further to 1543.0 nm and 1569.2 nm, respectively, under 840 mA excitation. Similar red-shift behaviours have also been observed for other lasing or non-lasing WGMs as the pump intensities increased from 100 mA to 910 mA and this for every concentration doping rate. It should be noted that all WGMs shift by 0.8 nm towards longer wavelength.

3. CAVITY TEMPERATURE EFFECT

The aim of this section is to develop the connection between the temperature rise and the line shift which happens when the pumping is increased. For this purpose, we firstly formulate the lasing wavelength shift in terms of the cavity temperature rise based on the lasing condition; then the cavity temperature is scaled by using the intensity ratio between two green upconversion emission.

3.1. Basic formulation of cavity thermal effect

The microspherical laser consists of an active cavity within which phonons associated with the non radiative decay between the manifolds of Erbium ions,*e.g.*,$^4I_{11/2} \longrightarrow^4 I_{13/2}$, and between the intra-Stark levels of the laser manifolds,*i.e.*, $^4I_{15/2}$ and $^4I_{13/2}$, create thermal deposition and thus heat the microsphere. An increase of cavity temperature $\triangle T$ results not only in a longitudinal expansion Δd of the microchip cavity but also in a change of index of refraction Δn. Both changes then affect the lasing condition and the wavelength shift $\triangle\lambda$ of every WGM as the cavity temperature rises by $\triangle T$ can be written as[18]

$$\triangle\lambda = \lambda \cdot (\frac{1}{n} \cdot \frac{\partial n}{\partial T} + \frac{1}{d} \cdot \frac{\partial d}{\partial T}) \cdot \triangle T \tag{3}$$

Here n and d are constant values which are referenced to the room temperature, or if one wants to be more precise, to the temperature corresponding to the threshold for oscillation. $\partial n/\partial T$,$\partial d/\partial T$ are change ratio with respect to temperature for the index of refraction and thermal expansion of the Er:ZBLALiP glasses.

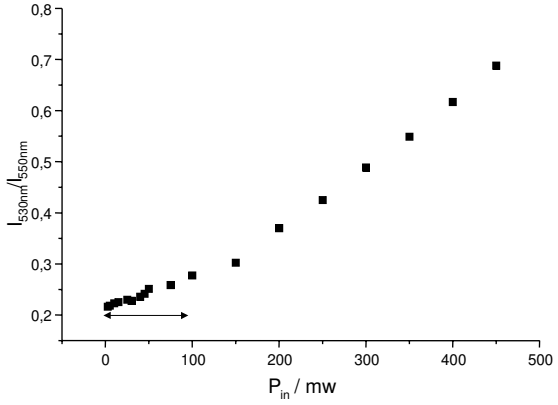

Figure 7. Dependence of the green emission intensity ratio *vs* incident pump power. Arrow corresponds to the pump power used here for laser oscillation

3.2. Thermal effect

To Calibrate the cavity temperature we use the upconversion intensity ratio originated from the levels $^4S_{3/2}$ (level 2) and $^2H_{11/2}$ (level 3) which are responsible for the green emission (Fig.7). Each green fluorescence spectrum can be decomposed into five Gaussian profiles by a Multi-Gaussian-Fit procedure. The peak wavelengths of these five Gaussian profiles remain quasi-independent of the incident pumping power, being 518.7 nm, 522.0 nm, 527.4 nm, 541.6 nm and 550.4 nm, respectively, while their height and area are different as the pumping power is increased. The physical mechansim is the same as described in ref.18 The multiphonon relaxation rate is inversely proportional to the number of phonons N necessary to span the energy gap between the $^4S_{3/2}$ and $^4F_{9/2}$. In reality, the energy gap between the levels of 2 and 3 is about 800 cm^{-1}, comparable to the value of $k_BT \approx 200\ cm^{-1}$, and much less than the energy gap between them and the nearest lower level $^4F_{9/2}$, about 3200 cm^{-1}(at least seven phonons to bridge this energy gap). This fact leads to a quasi-thermal population distribution in the manifolds of 2 and 3 due to strong phonon interaction(typically incorporating one or two phonons) between them. The ratio of the emission intensities originating from the levels 3 and 2 can thus be expressed by the following equation

$$\frac{I_3}{I_2} = \frac{A_3 g_3 h\nu_3}{A_2 g_2 h\nu_2} \cdot \exp[-\frac{E_{32}}{kT}] \tag{4}$$

where ν_2 and ν_3 are green emission frequencies, g_2 and g_3 the degeneracies $(2J+1)$ and A_2, A_3 the total spontaneous-emission rates of the level 2 and 3. E_{32} is the energy gap between the levels 2 and 3. An effective temperature T can now be evaluated in substituting spectroscopic data of Er:ZBLA glasses[19] into Equ.4

$$T = \frac{1152}{\ln(10.7) - \ln[I_3/I_2]} \tag{5}$$

A 2 $mol.\%$ Er:ZBLALiP microsphere 60 μm in diameter was used to scale cavity temperature due to its intense upconversion emission. In Figure 8, the green emission spectra attributed to the transitions from the metastable levels 3 and 2 to the fundamental level $^4I_{15/2}$ of Erbium ions are shown for 200 mA and 910 mA excitation. The central wavelengths of these two bands are 526 nm and 550 nm, respectively, which are calculated by weighting the Stoke's shifts. Introducing the intensity ratio between them in equation 5 lead to microsphere temperature of 327.6 K and 394.5 K, respectively, corresponding to a temperature rise of 66.9 K. This results in a red-shift

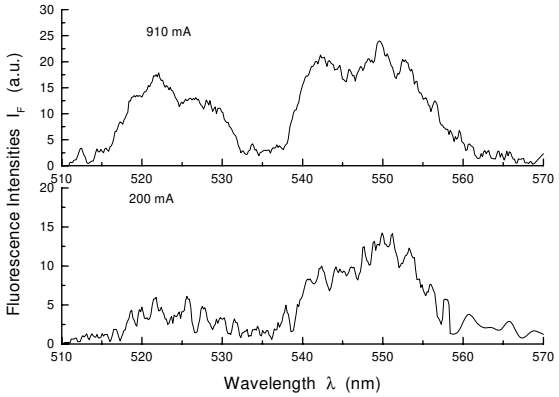

Figure 8: Green upconversion spectra for Er :ZBLALiP glass under $200mA$ and $910mA$ diode driving current

rate of 0.012 nm/K for Er:ZBLALiP glass. From equation 3, we yield

$$(\frac{1}{n}\cdot\frac{\partial n}{\partial T}+\frac{1}{d}\cdot\frac{\partial d}{\partial T})=78\times10^{-7}/K \tag{6}$$

For most ZBLA glasses, $\partial n/\partial T$ is only about one tenth of $\partial d/\partial T$ and generally the former is negative. If this hypothesis is assumed, $\partial d/\partial T=87\times10^{-7}/K$, and $\partial n/\partial T=-9\times10^{-7}/K$, which are similar to $84\times10^{-7}/K$ and $-10\times10^{-7}/K$ of QX-Kigre phosphate glass in the same temperature range.

4. CONCLUSION

A fluoride glass with composition revealing a high stability, with a weak nucleation tendency, has been studied. High optical quality microspheres have been made using a plasma torch. Er:ZBLALiP microsphere 1550 nm lasers have been achieved for several doping rates under pumping at 1480 nm. Red-shift effects of WGMs in Er:ZBLALiP microspheres with an increasing pump power was observed. A simple model based on the intensity ratio between two green upconversion emissions is proposed to interpret the thermal effect and to scale the cavity temperature rise. The result indicates that a 0.8 nm red-shift corresponds to 66.9 K temperature rise. Another prospective application is to construct a point temperature sensor by tens micrometer-size with fiber-coupled microspheres. Moreover, Von Klitzing[20]has recently demonstrated tuning ability of silica microspheres by 1 nm at 800 nm of WGMs with strain tuning method. In this paper we propose an alternative tuning technique based on inherent thermal expansion to realize a tunable range of 0.8 nm.

ACKNOWLEDGMENTS

This work is partially supported by a project of Chinese National Natural Scientific Foundation(CNNSF). One of our authors(ZPC), acknowledges le Ministère de l'Education Nationale, de la Recherche et de la Technologie(MENRT) for post-doctoral research program support. The authors thank Dr. M. Thual for the realization of half-tapers.

REFERENCES

1. M. Pollnau, S.D. Jackson, *IEEE-Journal of selected topics in quantum electronics***7**,p. 30, 2001.
2. R.K. Chang, A.J. Campillo, *Optical processes in microcavities*, World Scientific, Singapore, 1996.

3. L. Collot, V. Lefèvre-Seguin, M. Brune, J.M. Raimond, S. Haroche, *Europhys. Lett.* **23**,p. 327, 1993.
4. B.E. Little, J.P. Laine, D.R. Lim, H.A. Haus, L.C. Kimerling, S.T. Chu, *Opt. Lett.***25**,p. 73, 2000.
5. K. Miura, K. Tanaka, K. Hirao, *J. Mat. Sci. Lett.* **15**, p.1854, 1996.
6. V.S. Sandoghdar, F. Treussart, J. Hare, V. Lefèvre-Seguin, J.M. Raimond, S. Haroche,*Phys. Rev. A* **54**, p.1777, 1996.
7. F. Lissillour, P. Féron, N. Dubreuil, P. Dupriez, M. Poulain, G. Stéphan,*Elect. Lett.* **36**, p.1382, 2000.
8. M. Mortier, P. Goldner, P. Féron, G.M. Stéphan, H. Xu, Z. Cai, *J. Non Cryst. Solids* to be published.
9. D.E. McCumber,*Phys.Rev.*,**134**, p.299, 1964.
10. Y.D. Huang, M. Mortier, F. Auzel, *Optical Materials* **15**, p. 243, 2001.
11. S. Taccheo, P. Laporta, C. Svelto,*Appl.Phys.Lett.***68**, pp. 2621–2623, 1996.
12. M. Cai, O. Painter, K.J. Vahala, P.C. Sercel,*Opt. Lett.* **25**, p.1430, 2000.
13. M. Cai, K.J. Vahala,*Opt. Lett.***26**, pp. 884–886, 2001.
14. F. Lissillour, D. Messager, G.M. Stéphan, P. Féron, *Opt. Lett.***26**,pp. 1051–1053, 2001.
15. F. Lissillour, R. Gabet, P. Féron,P. Besnard, G.M. Stéphan, *Europhys. Lett.***55(4)**,pp. 499–504, 2001.
16. M.J.F. Digonnet,*Rare earth doped fiber lasers and amplifiers*, Stanford University, USA, 1993.
17. S. Schiller, R.L. Byer, *Opt. Lett.***16**, p.1138, 1991.
18. Z.P. Cai, A. Chardon, H.Y. Xu, P. Féron, G.M. Stéphan, *Opt. Comm.*,p. 301, 2002.
19. M.D. Shinn, W.A. Sibley, M.G. Drexhage, R.N. Brown, *Phys.Rev.B* **27**, p.6635, 1983.
20. W. von Klitzing, R. Long, V.S. Ilchenko, J. Hare, V. Lefèvre-Seguin, *Opt. Lett.***26**, pp. 166–168, 2001.